



Published by SET Publisher

Journal of Basic & Applied Sciences

ISSN (online): 1927-5129



Ambipolar Charge Transport of PCNTC-O and PCNTC-R Cocrystals Obtained Under 1:2 and 1:1 Ratios of Donor and Acceptor

Junle Ren^{1,2}, Zhelin Ding^{1,2}, Yuyao Li^{1,2}, Qiqi Mu^{1,2}, Qiguang Shen^{1,2}, Shoufeng Zhang^{1,*} and Li Zhang^{1,*}

¹School of Electronic Engineering, Guangxi University of Science and Technology, Liuzhou 545000, Guangxi, China

²School of Automation, Guangxi University of Science and Technology, Liuzhou 545000, Guangxi, China

Article Info:

Keywords:

Charge transport,
Bipolar organic semiconductors,
D-A cocrystal.

Timeline:

Received: November 05, 2022
Accepted: December 10, 2022
Published: December 26, 2022

Citation: Ren J, Ding Z, Li Y, Mu Q, Shen Q, Zhang S, Zhang L. Ambipolar charge transport of PCNTC-O and PCNTC-R cocrystals obtained under 1:2 and 1:1 ratios of donor and acceptor. J Basic Appl Sci 2022; 18: 147-157.

Abstract:

The efficiency of microelectronic devices depends greatly on the charge transport performance of organic semiconductors. The purpose of this work is to analyze the effect of donor-acceptor (D-A) cocrystals on the charge transport characteristics of organic semiconductors using the Marcus theory of electron transfer combined with kinetic Monte Carlo simulations. For two different cocrystals, sesquikis (benzene-1,2,4,5-tetracarboxitrile 2-(1,3-benzothiazol-2-yl)-3-(pyren-1-yl)prop-2-enenitrile(PCNTC-O) and ben-zene-1,2,4,5-tetracarboxitrile 2-(1,3-benzothiazol-2-yl)-3-(pyren-1-yl)pr-op-2-enenitrile(PCNTC-R) cocrystals, were investigated using 2-(benzo[d]-thiazol-2-yl)-3-(pyren-1-yl)acrylonitrile (Py-BZTCN) as the donor and 1,2,4,5-tetracyanobenzene (TCNB) as the acceptor mixed at 1:2 and 1:1 ratios, respectively. According to our calculations, PCNTC-O and PCNTC-R both exhibit bipolar charge transport behaviour with mobilities electron/hole attaining 0.0104/0.1252 and 0.0241/0.0598 cm²/Vs, respectively.

DOI: <https://doi.org/10.29169/1927-5129.2022.18.15>

*Corresponding Author

E-mail: zhangsf@gxust.edu.cn, zhangli@gxust.edu.cn

© 2022 Kara *et al.*; Licensee SET Publisher.

This is an open access article licensed under the terms of the Creative Commons Attribution Non-Commercial License (<http://creativecommons.org/licenses/by-nc/3.0/>) which permits unrestricted, non-commercial use, distribution and reproduction in any medium, provided the work is properly cited.

1. INTRODUCTION

Organic semiconducting materials have attracted a great deal of attention in the last few decades as the basic building block of organic electronic devices. Nowadays, organic light-emitting diodes (OLEDs) [1-4], organic field effect transistors (OFETs) [5-10] and organic photovoltaic (OPVs) [11-15] based on organic semiconductor materials are constantly coming into the limelight, making organic semiconductor materials promising for use in modern microelectronic devices. Improving charge transport in organic semiconductors is thus an important method for improving the efficiency of microelectronics devices.

Organic semiconductors can be classified into unipolar and bipolar materials depending on the type of carrier operation. Unipolar includes p-type where the carriers are holes and n-type where the carriers are electrons. Liu and co-workers reported the presence of 2,6-diphenylanthracene with a mobility of $34 \text{ cm}^2/\text{Vs}$ for p-type organic semiconducting materials [16]. Yamaguchi and co-workers reported S-shaped dinaphtho[2,1-b:2',1'-f]thieno[3,2-b]thiophene with a mobility of $11 \text{ cm}^2/\text{Vs}$ [17], both showing excellent hole mobilities. The highest mobility of tetrachlorinated diperylene bisimide has been reported by Lv and co-workers to reach $4.65 \text{ cm}^2/\text{Vs}$ [18] for n-type organic semiconducting materials, Li *et al.* reported fullerenes with mobility $11 \text{ cm}^2/\text{Vs}$ [19], exhibits good electron mobility.

Compared with unipolar organic semiconductor materials, bipolar organic semiconductor materials have the advantages of simple preparation process,

low production cost, low energy consumption, low noise, stable operation and so on, which is why we have to develop bipolar organic semiconductor materials. Huge progress has been made in recent years in the study of organic semiconducting bipolar materials, Compounds synthesized from triphenylamine and pyrimidine-5-carbon-itrile reported by and coworkers have an electron and hole mobilities of 4.4×10^{-4} and $7.3 \times 10^{-3} \text{ cm}^2/\text{Vs}$, respectively [20]. Currently, donor-acceptor complexes (D-A) have emerged as an efficient way to design and synthesize bipolar charge transport systems. The D-A complexes consisting of the meso-diphenyl tetrathia [22] annulene [2,1,2,1] as the donor molecule and 2,5-difluoro-7,7,8,8-tetracyanoquinodimethane as the acceptor molecule reported by and co-workers were found to have excellent bipolar charge transport with a mobility of 0.47 and $1.57 \text{ cm}^2/\text{Vs}$ for electrons and holes, respectively [21]. In addition, an increasing number of D-A complexes have been reported, showing good bipolar charge transport [22-31].

The charge transport properties of PCNTC-O and PCNTC-R formed from Py-BZTCN as the donor molecule and TCNB as the acceptor molecule were analyzed in a ratio of 1:2 and 1:1 (see Figure 1), which have been synthesized experimentally by Zhang and co-workers [32] and are shown in Table 1. In this work, we have characterized the charge transport performance of PCNTC-O and PCNTC-R in a mechanistic manner using Marcus electron transfer theory combined with kinetic Monte Carlo simulations, the results of our calculations show that PCNTC-O and PCNTC-R both exhibit good bipolar charge transport.

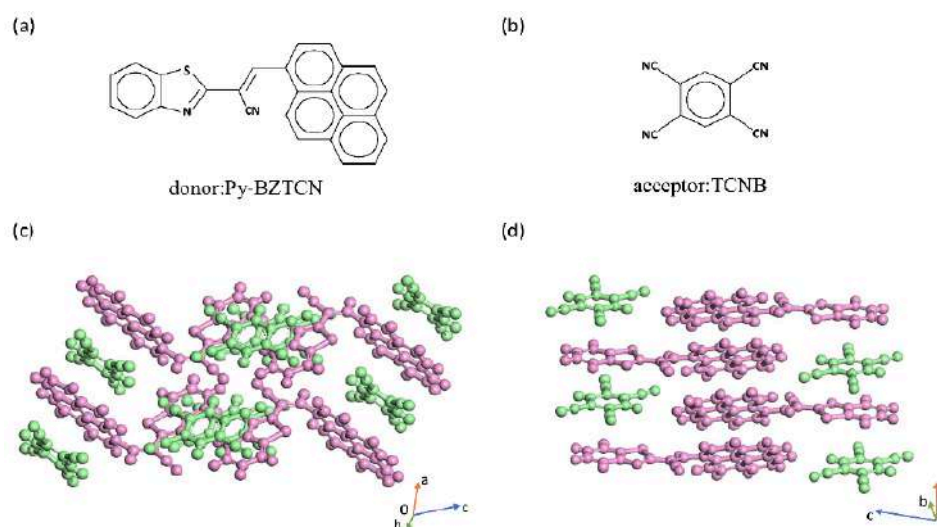


Figure 1: Chemical structures of (a) Py-BZTCN and (b) TCNB, the molecular structure of (c) PCNTC-O and (d) PCNTC-R cocrystals.

2. METHODOLOGY

We have used Marcus electron transfer theory in combination with kinetic Monte Carlo simulations to describe the properties of charge transport in this work. The charge transfer rate equation can be expressed as:

$$K_{CT} = \frac{1}{\hbar^2} |V|^2 \sqrt{\frac{\pi}{\lambda k_B T}} \exp\left(-\frac{\Delta G_0 + \lambda}{4k_B T}\right) \quad \# \quad (1)$$

Here, V is the electron transfer integral and λ is the reorganization energy resulting from the charge transfer process, ΔG_0 is the change in free energy before and after the reaction.

It can be seen that the electron transfer integral and the reorganization energy are two important parameters that determine the charge transfer rate. The direct coupling method for calculating the transfer integral between adjacent molecules can be expressed as:

$$V_{if} = \langle \varphi_i^0 | \hat{f} | \varphi_f^0 \rangle \quad \# \quad (2)$$

Here, \hat{f} is the Fock operator of a pair of molecules, φ_i^0 and φ_f^0 are the molecular orbitals of two molecules without perturbation, two orbitals are electron coupled for hole transport when they are HOMO and electron transport when they are LUMO. The transfer integral is closely related to spatial factors such as relative distance and angle between a pair of neighboring molecules, which means that the charge transfer rate is directly related to the molecular stacking mode.

For reorganization energy, there are two methods of calculation, the first is the adiabatic potential energy surface method can be expressed as:

$$\lambda = \lambda_1 + \lambda_2 \quad (3)$$

Where λ_1 is the geometric relaxation energy corresponding to the loss of a hole or electron from the ionic state molecule to the neutral state, and λ_2 is the geometric relaxation energy corresponding to the gain of a hole or electron from the neutral state molecule to the ionic state (see Figure S1). The second is the normal mode method can be expressed as:

$$\lambda = \sum_j \lambda_j = \sum_j S_j \hbar \omega_j \quad \# \quad (4)$$

Here, $S_j = \lambda_j / \hbar \omega_j$ is the Huang–Rhys factor, which describes the strength of electron-phonon coupling, ω_j is the vibration frequency in the j th normal mode, reorganization energy can be divided into the contribution of each vibration mode.

The charge mobility can be obtained by the Einstein relation:

$$\mu = \frac{eD}{k_B T} \quad \# \quad (5)$$

Here, D is the diffusion coefficient of the charge, which can be expressed as:

$$D = \lim_{t \rightarrow \infty} \frac{x(t)^2}{2nt} \quad \# \quad (6)$$

Here, $x(t)$ is the distance of charge transport, t is the diffusion time and n is the dimension of charge transport. The diffusion coefficient can be obtained by a dynamic Monte Carlo simulation process, we arbitrarily choose a molecule as the starting point for a charge that can jump to the nearest surrounding molecule. The probability of following a particular transition path j can be calculated by $P_j = k_{CT}^j / \sum_j k_{CT}^j$, the distance of each jump is the central distance between two neighboring molecules, the jump time is $1/k_{CT}^j$. Before each jump of charge, a uniformly distributed random number r between 0 and 1 is randomly generated, if $\sum_{j=1}^{j-1} P_j < r < \sum_{j=1}^j P_j$, then the charge jumps to the j molecule, and the corresponding displacement and time are recorded. The diffusion coefficient is obtained by repeating the simulation process, which requires thousands of simulations to obtain a linear relationship between the mean square displacement and the simulation time. Finally, the mobility can be derived from Einstein relation. The calculations using the B3LYP function and the 6-31g* basis group.

3. RESULTS AND DISCUSSION

3.1. Electronic Structure

For PCNTC-O and PCNTC-R cocrystals, we calculated the frontier molecular orbitals using density functional theory (see Figure 2).

From Figure 2, we can see that the highest occupied molecular orbital (HOMO) in the PCNTC-O and PCNTC-R cocrystals is on the Py-BZTCN molecule, while the lowest unoccupied molecular orbital (LUMO) is on the TCNB molecule, indicating a significant charge transfer feature from the Py-BZTCN molecule to the TCNB molecule. For PCNTC-O cocrystal, the calculated energy levels of HOMO and LUMO are -6.03 eV and -3.52 eV, respectively. For PCNTC-R cocrystal, the calculated energy levels of HOMO and LUMO are -5.58 eV and -3.58 eV, respectively. It can be seen that the energy gap of the PCNTC-R cocrystal is narrower than that of the PCNTC-O cocrystal because the Py-BZTCN molecule in the PCNTC-O cocrystal is twisted

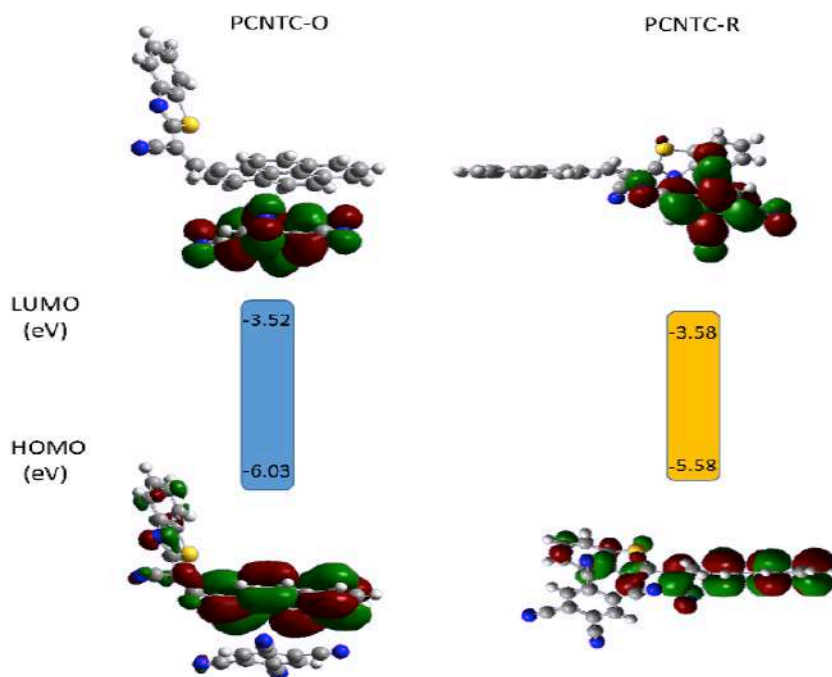


Figure 2: Electron distribution of the HOMO and LUMO of PCNTC-O and PCNTC-R cocrystals.

at a larger angle, while the Py-BZTCN molecule in the PCNTC-R cocrystal is twisted at a smaller angle and is approximately a plane, so the PCNTC-R cocrystal has a better planar molecular skeleton with strong π - π interactions, and the parallel structure can effectively reduce the spatial site resistance, so the energy gap of HOMO-LUMO is reduced.

3.2. Reorganization Energy

Reorganization energy is one of the most important factors affecting carrier mobility and in this paper we have calculated the reorganization energy using normal mode analysis. In the PCNTC-O cocrystal, the Py-BZTCN molecule electron and hole duschinsky rotation

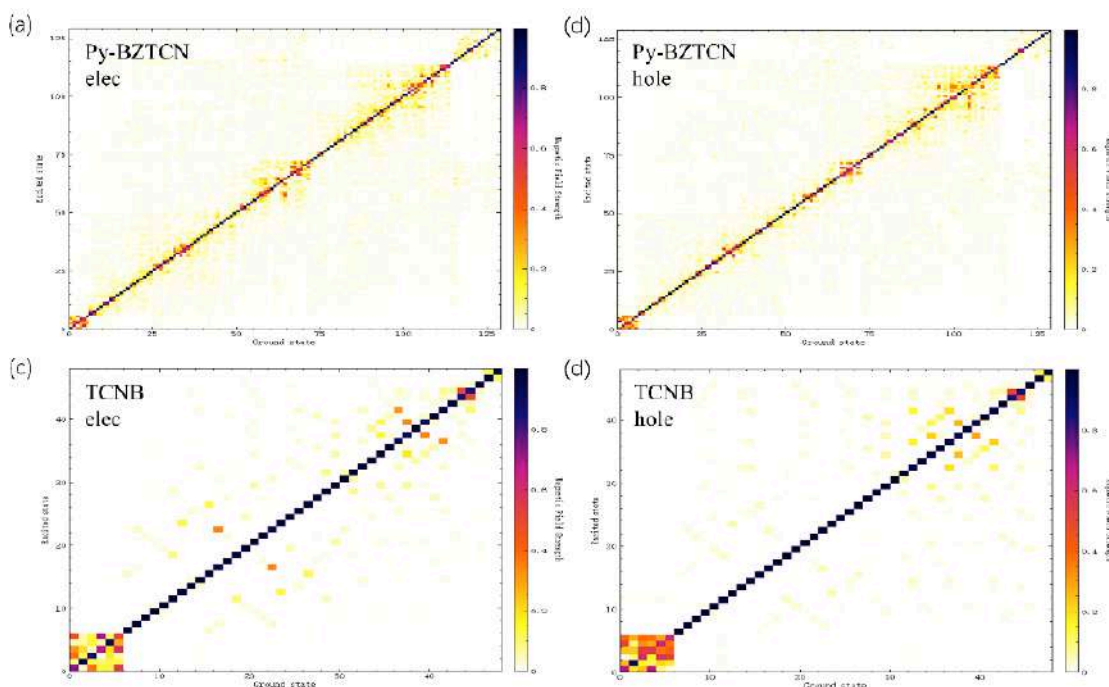


Figure 3: The Py-BZTCN molecule (a) electron and (b) hole duschinsky rotation matrix and TCNB molecule (c) electron and (d) hole duschinsky rotation matrix in PCNTC-O.

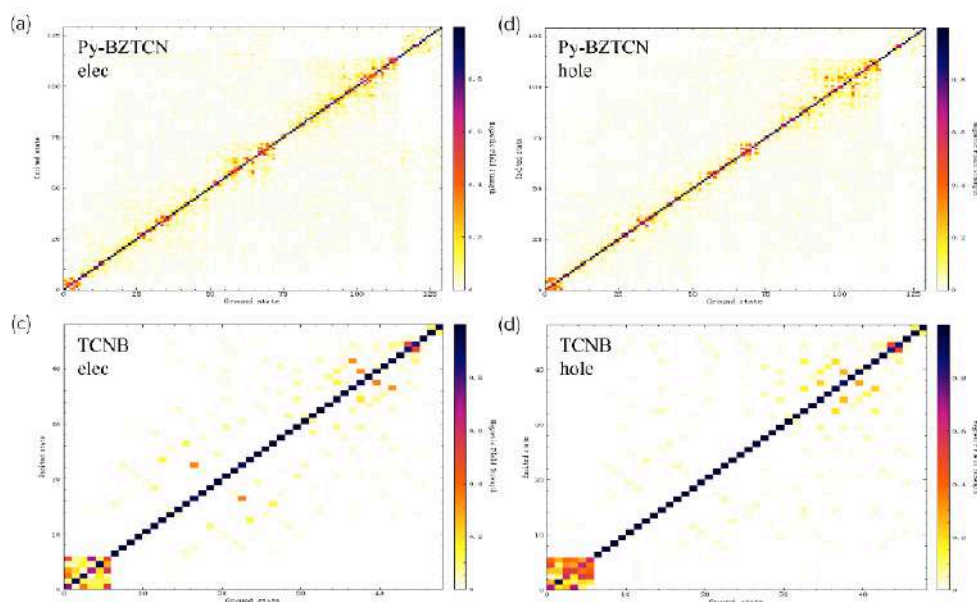


Figure 4: The Py-BZTCN molecule (a) electron and (b) hole duschinsky rotation matrix and TCNB molecule (c) electron and (d) hole duschinsky rotation matrix in PCNTC-R.

matrix and the TCNB molecule electron and hole duschinsky rotation matrix are shown in Figure 3.

In the PCNTC-R cocrystal, the Py-BZTCN molecule electron and hole duschinsky rotation matrix and the TCNB molecule electron and hole duschinsky rotation matrix are shown in Figure 4.

From the duschinsky rotation matrix we can see that Py-BZTCN is discrete while TCNB is linear, so we use the normal mode method to analyze the TCNB molecule reorganization energy.

In the PCNTC-O cocrystal, for the acceptor TCNB, the maximum electron reorganization energy the medium frequency region (see Figure 5), the maximum electron

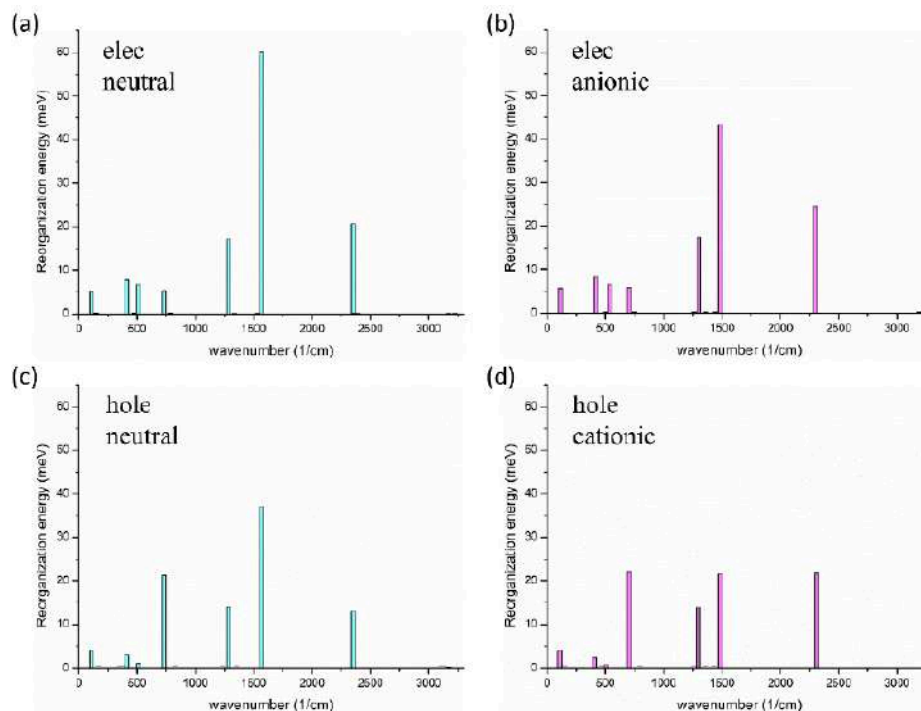


Figure 5: The contribution of the TCNB molecule electronic reorganization energy to each vibrational mode in the (a) neutral and (b) anionic states, and contribution of hole reorganization energy to each vibrational mode in the (c) neutral and (d) cationic states in PCNTC-O cocrystal.

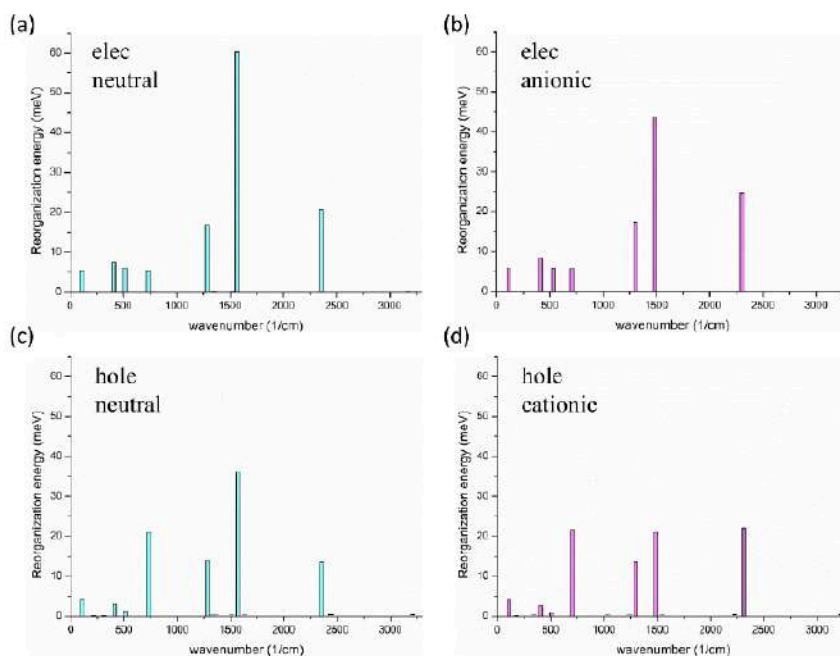


Figure 6: The contribution of the TCNB molecule electronic reorganization energy to each vibrational mode in the (a) neutral and (b) anionic states, and contribution of hole reorganization energy to each vibrational mode in the (c) neutral and (d) cationic states in PCNTC-R cocrystal.

Table 1: The TCNB Molecule Reorganization Energy of PCNTC-O and PCNTC-R Cocrystals

Reorganization energy (meV)		electronic	hole
PCNTC-O	TCNB	235.51	181.29
PCNTC-R	TCNB	233.34	178.81

reorganization energy in neutral state reaches 60.24 meV at a frequency of 1568.70 cm^{-1} and in anionic state reaches 43.32 meV at a frequency of 1484.40 cm^{-1} , this is mainly due to C atoms in the benzene ring from upward and downward motion (the molecular vibration diagram is shown in Figure S2). The maximum hole reorganization energy in the neutral state reaches 37.20 meV at a frequency of 1568.70 cm^{-1} , while in the cationic state the maximum reorganization energy reaches 22.09 meV at frequency of 705.91 cm^{-1} , this is mainly due to the forward and backward motion of the C atom on the TCNB molecule. The large electron reorganization energy of TCNB molecule will have a negative impact on electron mobility.

In the PCNTC-R cocrystal, for the acceptor TCNB, the maximum electron reorganization energy reaches a maximum in the medium frequency region (see Figure 6), the maximum electron reorganization energy in the neutral state reaches 60.26 meV at a frequency of 1567.91 cm^{-1} and in the anionic state reaches 43.37 meV at a frequency of 1484.23 cm^{-1} , both due to the

upward and downward motion of the C atom on the benzene ring (the molecular vibration diagram is shown in Figure S3). The maximum hole reorganization energy in the neutral state reaches 36.13 meV at a frequency of 1567.91 cm^{-1} and the maximum hole reorganization energy in the cationic state reached 22.11 meV at a frequency of 2313.36 cm^{-1} , this is mainly due to the change of the C atom in the benzene ring from an upward and downward motion to an stretching motion of C and N atoms in cyano, the TCNB molecule reorganization energy calculation results are shown in Table 1.

3.3. Transfer Integral

The transfer integral is one of the most important factors affecting carrier mobility. The transfer integral is mainly influenced by spatial factors such as the relative distance and angle between neighbouring molecules, which means that the rate of charge transfer is directly related to the stacking pattern of the molecules. In this work, we have used the direct coupling method for the different paths of PCNTC-O and PCNTC-R cocrystal.

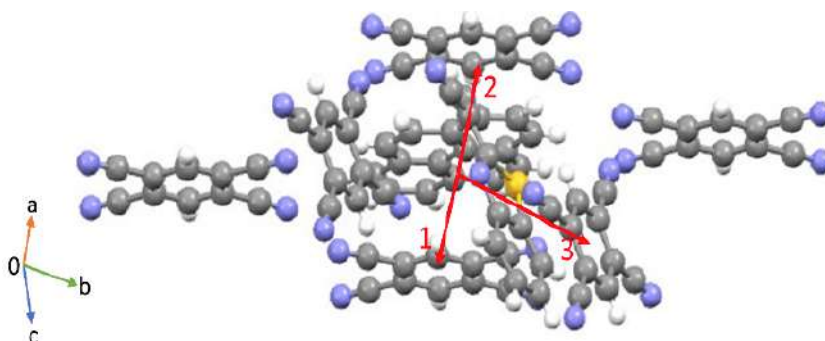


Figure 7: The most important charge hopping pathways for hole and electron in PCNTC-O cocrystal.

Table 2: The Most Important Transfer Integrals of Holes and Electrons in PCNTC-O Cocrystal

Transfer paths	Central distances (Å)	V_e (meV)	V_h (meV)
1	4.21	13.92	9.76
2	5.42	8.95	13.66
3	8.49	-40.65	9.72

For PCNTC-O cocrystal, we have studied the pathways with neighbouring molecules and the transfer integrals of electrons and holes, centred on the Py-BZTCN molecule, the most important charge hopping pathways given in Figure 7.

The most important transfer integrals of electrons and holes, as well as the intermolecular distances and intermolecular transfer paths are shown in Table 2. Large transfer integrals for hole are path 1 and path 2, this is because they are along the π -stacking direction

and these two molecules are in a parallel structure with the central molecule, which can effectively reduce the spatial site resistance and thus can produce a large hole transfer integral. In addition, the path 3 has a large hole transfer integral, as well as the transfer integral of electron reaches a maximum in the path 3, with a maximum value of -40.65 meV, this is mainly due to the large overlap of orbitals between the two molecules. In summary, the transfer integral for electrons is higher than holes.

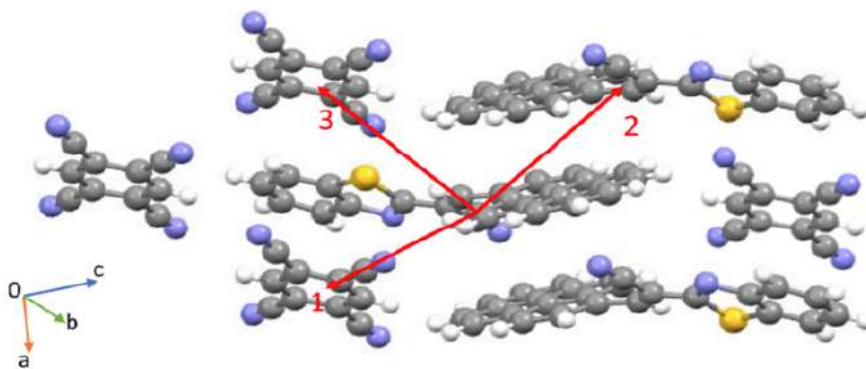


Figure 8: The most important charge hopping pathways for hole and electron in PCNTC-R cocrystal.

Table 3: The Most Important Transfer Integrals of Holes and Electrons in PCNTC-R Cocrystal

Transfer paths	Central distances (Å)	V_e (meV)	V_h (meV)
1	6.11	69.74	1.46
2	7.31	-56.21	-50.22
3	7.31	-57.82	5.91

Table 3 shows the most important transfer integrals of electrons and holes in the PCNTC-R cocrystal, the most important charge hopping paths given by Figure 8.

For the PCNTC-R cocrystal, the path 2 has the highest hole transfer integral at -50.222 meV, this path has a larger transfer integral than the other paths, due to the good parallelism and the large overlap area of the orbitals between the two neighbouring molecules. The transfer integrals of the electrons are larger for the paths 1, 2 and 3 and reach a maximum of 69.74 meV for the path 1, this is due to the path 1 has the shortest intermolecular distance and good π - π stacking, thus have a larger transfer integral. For the PCNTC-R cocrystal, the transfer integrals of both holes and electrons reach a relatively large value, which indicates that both holes and electrons have good mobility and therefore the PCNTC-R cocrystal may show a good bipolar transport.

3.4. Anisotropic Property

The anisotropic mobilities of PCNTC-O and PCNTC-R cocrystal have been calculated using kinetic Monte Carlo simulations. Firstly, for the PCNTC-O cocrystal,

the electron and hole mobilities were calculated from xy , xz and yz planes, respectively, and the xy plane result are shown in Figure 9 (xz and yz planes see Figure S4). For the electron mobility, there is a maximum on the xy plane along 110° and 290° , and the electron mobility reaches a maximum value of 0.017 cm^2/Vs on the xy plane. For the mobility of holes, it can be seen that there is a maximum mobility along 100° and 280° on the xy plane, with the maximum hole mobility reaching a maximum of 0.244 cm^2/Vs on the xy plane. As can be seen in Figure 9, the mobility of holes is an order of magnitude higher than that of electrons, although the transport performance for holes is better, but also shows ambipolar charge transport.

For the PCNTC-R cocrystal, we have also calculated the electron and hole mobilities on the xy , xz and yz planes and the xy plane result are shown in Figure 10 (xz and yz planes see Figure S5). Firstly, for the electron mobility, we can see that there is a maximum mobility along 170° and 350° on the xy plane. After our calculations, the electron mobility reaches a maximum value of 0.036 cm^2/Vs on the xy plane. For the mobility of holes, it can be seen that there is a maximum mobility along 70° and 250° on the xy plane, with the highest hole mobility reaching 0.119 cm^2/Vs on the xy

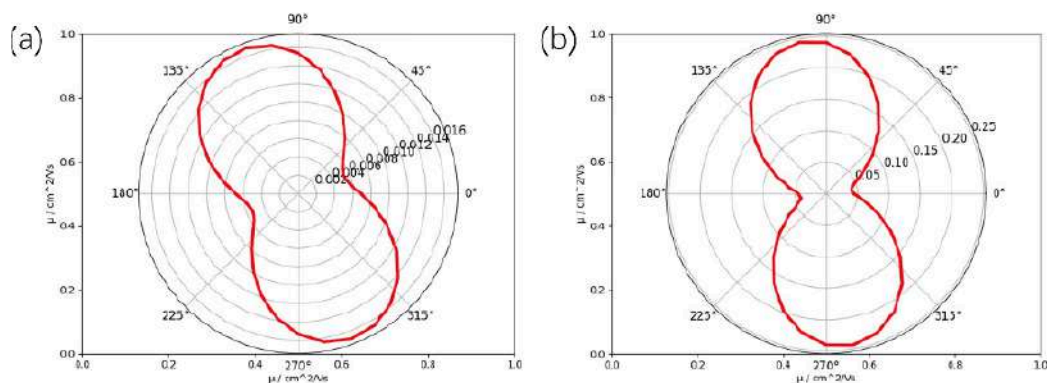


Figure 9: Mobility of electrons in the (a) xy and holes in the (b) xy planes in PCNTC-O cocrystal.

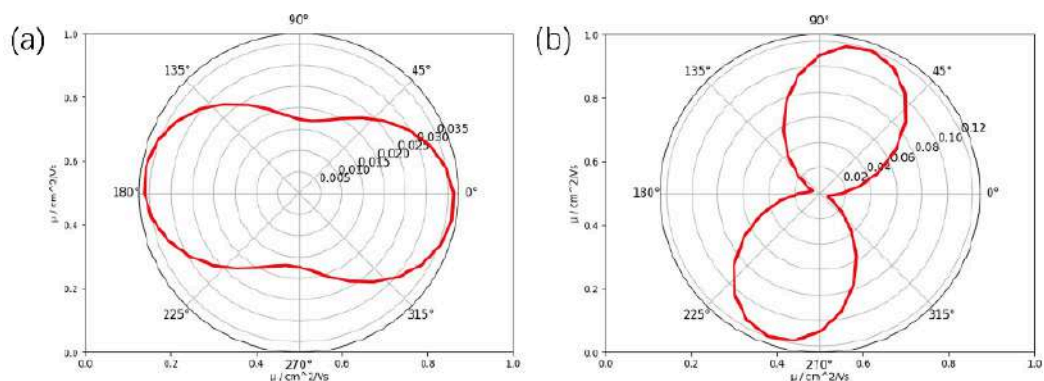
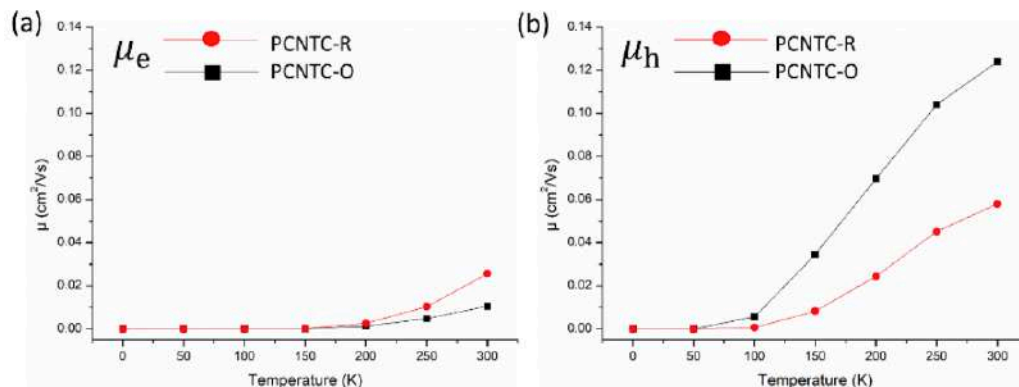


Figure 10: Mobility of electrons in the (a) xy and holes in the (b) xy plane in PCNTC-R cocrystal.

Table 4: The Average Carrier Mobilities of PCNTC-O and PCNTC-R Cocrysal

Mobility (cm^2/Vs)	μ_e	μ_h
PCNTC-O	0.0104	0.1252
PCNTC-R	0.0241	0.0598

**Figure 11:** PCNTC-O and PCNTC-R temperature dependences of the mobility of electrons (a) and holes (b)

plane. As can be seen in Figure 10, the PCNTC-R has a small difference in the mobility of holes and electrons and is able to show a good ambipolar charge transport.

The average carrier mobilities of PCNTC-O and PCNTC-R cocrysal are given in the Table 4. In PCNTC-O cocrysal composed in a 1:2 ratio of donor-acceptor, the average mobilities of electrons and holes is 0.0104 and 0.1252 cm^2/Vs respectively. Although the mobility of electrons is an order of magnitude smaller than the mobility of holes, it still shows ambipolar charge transport behavior. Compared to the PCNTC-O cocrysal, in PCNTC-R cocrysal composed in a 1:1 ratio of donor-acceptor, the average mobilities of electrons and holes is 0.0241 and 0.0598 cm^2/Vs respectively, which basically achieves a state of balanced electron and hole transport, showing an excellent ambipolar transport, probably because the energy gap in the PCNTC-R cocrysal is smaller than that in the PCNTC-O cocrysal, effectively increasing the carrier mobility.

3.5. Temperature Dependences of the Mobility

In addition, we have analyzed the effect of temperature changes on the mobility of PCNTC-O and PCNTC-R (see Figure 11).

From our calculations, it is clear that the mobility of both PCNTC-O and PCNTC-R increases with increasing temperature due to thermal activation process. As can be seen from Figure 11, the electron

mobility of PCNTC-R is higher than that of PCNTC-O as the temperature increases, while the hole mobility of PCNTC-O is higher than that of PCNTC-R. Overall both PCNTC-O and PCNTC-R have higher hole mobilities than electron mobilities.

4. CONCLUSION

In conclusion, we have investigated the PCNTC-O and PCNTC-R cocrysal formed with the donor molecule Py-BZTCN and the acceptor molecule TCNB in the ratios of 1:2 and 1:1. The carrier mobility of PCNTC-O and PCNTC-R cocrysal was calculated using Marcus electron transfer theory combined with kinetic Monte Carlo simulations. We analyzed two important factors affecting carrier mobility, reorganization energy and transfer integral, and found that the reorganization energy of electrons is higher than that of holes in PCNTC-O and PCNTC-R cocrysal, in addition, the transfer integral of PCNTC-R cocrysal is larger than that of PCNTC-O cocrysal from an overall perspective. In conclusion, we have shown that both PCNTC-O and PCNTC-R cocrysal exhibit ambipolar charge transport, compared to the PCNTC-O cocrysal, the And PCNTC-R cocrysal has a more balanced electron and hole mobility, demonstrating excellent charge transport properties of the bipolar type. This is due to the fact that the planarity of PCNTC-R cocrysal composed of 1:1 donor-acceptor is better than that of PCNTC-O cocrysal composed of 1:2 donor-acceptor. To conclude, the relationship between the crystal structure and charge transport has been studied in this

work, which is of great interest in designing high-performance organic devices with ambipolar charge transport.

ACKNOWLEDGEMENTS

This work was supported by the Natural Science Foundation of China (62105075) and Guangxi Department of Science and Technology (2020GXNSFBA159049, 2021GXNSFBA220021, AD19245107 and AD19110030).

SUPPORTING INFORMATION

The supporting information can be downloaded from the journal website along with the article.

REFERENCES

- [1] Luo Y, Li S, Zhao Y, *et al.* An Ultraviolet Thermally Activated Delayed Fluorescence OLED with Total External Quantum Efficiency over 9%[J]. *Advanced Materials* 2020; 32(32): 2001248. <https://doi.org/10.1002/adma.202001248>
- [2] Zoppi L, Martin-Samos L, Baldrige K. Effect of Molecular Packing on Corannulene Based Materials Electroluminescence[J]. *Journal of the American Chemical Society* 2011; 133: 14002-14009. <https://doi.org/10.1021/ja2040688>
- [3] Izawa S, Morimoto M, Naka S, *et al.* Spatial distribution of triplet excitons formed from charge transfer states at donor/acceptor interface[J]. *Journal of Materials Chemistry A*. 2022. <https://doi.org/10.1039/D2TA02068H>
- [4] Havare K. Effect of the interface improved by self-assembled aromatic organic semiconductor molecules on performance of OLED[J]. *ECS Journal of Solid State Science and Technology* 2020; 9(4): 041007. <https://doi.org/10.1149/2162-8777/ab8789>
- [5] Fu B, Hou X, Wang C, *et al.* A bowl-shaped sumanene derivative with dense convex-concave columnar packing for high-performance organic field-effect transistors[J]. *Chemical Communications* 2017; 53: 11407-11409. <https://doi.org/10.1039/C7CC05889F>
- [6] Shi K, Lei T, Pei J, A bowl-shaped molecule for organic field-effect transistors: crystal engineering and charge transport switching by oxygen doping[J]. *Chemical Science* 2014; 5: 1041-1045. <https://doi.org/10.1039/C3SC52701H>
- [7] Salunke K, Wong L, Feron K, *et al.* Phenothiazine and carbazole substituted pyrene based electroluminescent organic semiconductors for OLED devices[J]. *Journal of Materials Chemistry C* 2016; 4(5): 1009-1018. <https://doi.org/10.1039/C5TC03690A>
- [8] Chen R, Shi K, Wu F, *et al.* Corannulene derivatives with low LUMO levels and dense convex-concave packing for n-channel organic field-effect transistors[J]. *Chemical Communications* 2015; 51: 13768-13771. <https://doi.org/10.1039/C5CC03550C>
- [9] Zhang J, Liu G, Zhou Y, *et al.* Solvent accommodation: functionalities can be tailored through co-crystallization based on 1: 1 coronene-F4TCNQ charge-transfer complex[J]. *ACS Applied Materials & Interfaces* 2017; 9(2): 1183-1188. <https://doi.org/10.1021/acsami.6b15027>
- [10] Vegiraju S, Luo X, Li L, *et al.* Solution Processable Pseudo n-Thienoacenes via Intramolecular S···S Lock for High Performance Organic Field Effect Transistors[J]. *Chemistry of Materials* 2020; 32(4): 1422-1429. <https://doi.org/10.1021/acs.chemmater.9b03967>
- [11] Brabec J, Sariciftci S, Hummelen C. Plastic Solar Cells[J]. *Advanced Functional Materials* 2001; 11(1): 15-26. [https://doi.org/10.1002/1616-3028\(200102\)11:1<15::AID-ADFM15>3.0.CO;2-A](https://doi.org/10.1002/1616-3028(200102)11:1<15::AID-ADFM15>3.0.CO;2-A)
- [12] Li N, Baran D, Forberich K, *et al.* Towards 15% energy conversion efficiency: a systematic study of the solution-processed organic tandem solar cells based on commercially available materials[J]. *Energy & Environmental Science* 2013; 6(12): 3407-3413. <https://doi.org/10.1039/c3ee42307g>
- [13] Wu G, Zhang Y, Kaneko R, *et al.* Anthradithiophene based hole-transport material for efficient and stable perovskite solar cells[J]. *Journal of Energy Chemistry* 2020; 48: 293-298. <https://doi.org/10.1016/j.jechem.2020.02.021>
- [14] Yao L, Rahmanudin A, Guijarro N, *et al.* Organic semiconductor based devices for solar water splitting[J]. *Advanced Energy Materials* 2018; 8(32): 1802585. <https://doi.org/10.1002/aenm.201802585>
- [15] Liu S, Li C, Xu X, *et al.* Efficiency enhancement of organic photovoltaics by introducing high-mobility curved small-molecule semiconductors as additives[J]. *Journal of Materials Chemistry A* 2019; 7(20): 12740-12750. <https://doi.org/10.1039/C9TA02636C>
- [16] Liu J, Zhang H, Dong H, *et al.* High mobility emissive organic semiconductor[J]. *Nature Communications* 2015; 6(1): 10032. <https://doi.org/10.1038/ncomms10032>
- [17] Yamaguchi Y, Kojiguchi Y, Kawata S, *et al.* Solution-Processable Organic Semiconductors Featuring S-Shaped Dinaphthothienothiophene (S-DNTT): Effects of Alkyl Chain Length on Self-Organization and Carrier Transport Properties[J]. *Chemistry of Materials* 2020; 32(12): 5350-5360. <https://doi.org/10.1021/acs.chemmater.0c01740>
- [18] Lv A, Puniredd S R, Zhang J, *et al.* High mobility, air stable, organic single crystal transistors of an n-type diperylene bisimide[J]. *Advanced Materials* 2012; 24(19): 2626-2630. <https://doi.org/10.1002/adma.201104987>
- [19] Li H, Tee BCK, Cha JJ, *et al.* High-mobility field-effect transistors from large-area Solution-grown aligned C60 single crystals[J]. *Journal of the American Chemical Society* 2012; 134(5): 2760-2765. <https://doi.org/10.1021/ja210430b>
- [20] Tsiko U, Volyniuk D, Andruleviciene V, *et al.* Triphenylamino or 9-phenyl carbazolyl-substituted pyrimidine-5-carbonitriles as bipolar emitters and hosts with triplet harvesting abilities[J]. *Materials Today Chemistry* 2022; 25: 100955. <https://doi.org/10.1016/j.mtchem.2022.100955>
- [21] Qin Y, Cheng C, Geng H, *et al.* Efficient ambipolar transport properties in alternate stacking donor-acceptor complexes: from experiment to theory[J]. *Physical Chemistry Chemical Physics* 2016; 18(20): 14094-14103. <https://doi.org/10.1039/C6CP01509C>
- [22] Jin J, Long G, Gao Y, *et al.* Supramolecular Design of Donor-Acceptor Complexes via Heteroatom Replacement toward Structure and Electrical Transporting Property Tailoring[J]. *ACS Appl. Mater Interfaces* 2019; 11: 1109-1116. <https://doi.org/10.1021/acsami.8b16561>
- [23] Mandal A, Swain P, Nath B, *et al.* Unipolar to ambipolar semiconductivity switching in charge transfer cocrystals of 2,7-di-tert-butylpyrene[J]. *Cryst Eng Comm* 2019; 21: 981-989. <https://doi.org/10.1039/C8CE01806E>

- [24] Iijima K, Sanada R, Yoo D, *et al.* Carrier Charge Polarity in Mixed-Stack Charge-Transfer Crystals Containing Dithienobenzodithiophene[J]. ACS Appl Mater Interfaces 2018; 10: 10262-10269. <https://doi.org/10.1021/acsami.8b00416>
- [25] Sato R, Dogishi M, Higashino T, *et al.* Charge-Transfer Complexes of Benzothienobenzothio-phene with Tetracyanoquinodimethane and the n-Channel Organic Field-Effect Transistors[J]. The Journal of Physical Chemistry C 2017; 121: 6561-6568. <https://doi.org/10.1021/acs.jpcc.7b00902>
- [26] Hu P, Li H, Li Y, *et al.* Single-crystal growth, structures, charge transfer and transport properties of anthracene-F4TCNQ and tetracene-F4TCNQ charge-transfer compounds[J]. Cryst Eng Comm 2017; 19: 618-624. <https://doi.org/10.1039/C6CE02116F>
- [27] Zhang J, Gu P, Long G, *et al.* Switching charge-transfer characteristics from p-type to n-type through molecular "doping" (co-crystallization) [J]. Chemical Science 2016; 7: 3851-3856. <https://doi.org/10.1039/C5SC04954G>
- [28] Higashino T, Dogishi M, Kadoya T, *et al.* Air-stable n-channel organic field-effect transistors based on charge-transfer complexes including dimethoxybenzothienobenzothiophene and tetracyanoquinodimethane derivatives[J]. Journal of Materials Chemistry C 2016; 4: 5981-5987. <https://doi.org/10.1039/C6TC01532H>
- [29] Zhu W, Yi Y, Zhen Y, *et al.* Precisely Tailoring the Stoichiometric Stacking of Perylene-TCNQ Co-Crystals towards Different Nano and Microstructures with Varied Optoelectronic Performances[J]. Small 2015; 11: 2150-2156. <https://doi.org/10.1002/sml.201402330>
- [30] Tsutsumi J, Matsuoka S, Inoue S, *et al.* N-Type Field-Effect Transistor Based on Layered Crystalline Donor-Acceptor Semiconductors with Dialkylated Benzothienobenzothiophenes as Electron Donors[J]. Journal of Materials Chemistry C 2015; 3: 1976-1981. <https://doi.org/10.1039/C4TC02481H>
- [31] Su Y, Li Y, Liu J, *et al.* Donor-acceptor cocrystal based on hexakis(alkoxy)triphenylene and perylenediimide derivatives with an ambipolar transporting property[J]. Nanoscale 2015; 7: 1944-1955. <https://doi.org/10.1039/C4NR05915H>
- [32] Zhang X, De J, Liu H, *et al.* Cis-Trans Isomerism Inducing Cocrystal Polymorphism with Thermally Activated Delayed Fluorescence and Two-Photon Absorption[J]. Advance Optical Materials 2022; 2200286. <https://doi.org/10.1002/adom.202200286>